Available online at www.sciencedirect.com
ScienceDirect
Journal of Sound and Vibration 306 (2007) 495–506
JOURNAL OF SOUND AND VIBRATION
www.elsevier.com/locate/jsvi

Flexural–torsional-coupled vibration analysis of axially loaded closed-section composite Timoshenko beam by using DTM

M.O. Kaya*, O. Ozdemir Ozgumus

Faculty of Aeronautics and Astronautics, Istanbul Technical University, 34469 Istanbul, Turkey

Received 19 July 2005; received in revised form 8 January 2007; accepted 9 May 2007
Available online 30 July 2007

Abstract

This study introduces the differential transform method (DTM) to analyse the free vibration response of an axially loaded, closed-section composite Timoshenko beam which features material coupling between flapwise bending and torsional vibrations due to ply orientation. The governing differential equations of motion are derived using Hamilton's principle and solved by applying DTM. The mode shapes are plotted, the natural frequencies are calculated and the effects of the bending–torsion coupling, the axial force and the slenderness ratio on the natural frequencies are investigated using the computer package, Mathematica. Wherever possible, comparisons are made with the studies in open literature.

1. Introduction

Composite materials are increasingly being preferred in the construction of aerospace structures such as aircraft wings and helicopter blades. These materials have favourable engineering properties such as high strength/stiffness to weight ratios and excellent fatigue behaviour [1]. Another advantage of the composite structures is its ability to be controlled of the structural properties such as elastic and structural couplings through the use of specific lay-up and fibre orientations.

Due to their practical importance and potential benefits mentioned above, the vibration analysis of composite beams has been an important research area in recent years. The coupling between the bending and torsional vibrations, which can occur in both solid and thin-walled composite beams, is of particular interest from an aeroelastic standpoint [2]. Bank and Kao [3] analysed free and forced vibration of thin-walled fibre-reinforced composite material beams using the Timoshenko beam theory. Song and Librescu [4] worked on the study of the bending vibration response of laminated composite cantilevered thin-walled box beam subjected to a harmonically oscillatory concentrated load. Rao and Ganesan [5] examined the harmonic response of tapered composite beams by using a finite element model based on the higher-order shear deformation theory. Banerjee [6] used the dynamic stiffness matrix method to study the free vibration behaviour of an axially loaded composite Timoshenko beam. Na and Librescu [7] investigated a number of

*Corresponding author. Tel.: +90 212 285 31 10; fax: +90 212 285 29 26.
E-mail address: kayam@itu.edu.tr (M.O. Kaya).

0022-460X/$ - see front matter
doi:10.1016/j.jsv.2007.05.049

effects that are geometric and physical in nature on the dynamic response control of adaptive nonuniform composite thin-walled beams.

In this study, which is an extension of the authors' previous works [8–10], vibration analysis of an axially loaded, composite Timoshenko beam with bending–torsion coupling is performed using the differential transform method (DTM). The concept of this method was first introduced by Zhou [11] in 1986 and it was used to solve both linear and nonlinear initial value problems in electric circuit analysis. The method has the inherent ability to deal with nonlinear problems which enabled Chiou and Tzeng [12] to apply the Taylor transform to solve nonlinear vibration problems. Furthermore, the method may be employed for the solution of both ordinary and partial differential equations. Jang et al. [13] applied the two-dimensional DTM to the solution of partial differential equations. Abdel and Hassan [14] adopted the differential transformation method to solve some eigenvalue problems. Since previous studies have shown that the DTM to be an efficient tool to solve nonlinear or parameter varying systems, it is not surprising that it has gained much attention of several researchers [15–18], in recent years.

2. Formulation

A straight composite beam with length L, height h and breadth b is shown in Fig. 1. In the right-handed Cartesian coordinate system, the x-axis is the centroidal axis of the beam. The flexural displacement, $w(x,t)$ and the torsional rotation, $\psi(x,t)$ of the x-axis, occur in the z direction and about the x-axis itself, respectively. Here, x and t, respectively denote the spanwise coordinate and the time. Since the cross-sections of the beam have symmetry in both planes, the x-axis is also the locus of the geometric shear centres of the beam cross-sections. Therefore, the beam features material coupling between flapwise bending and torsional vibrations only due to ply orientation. The constant axial force P, which acts through the centroid of the cross section, is considered to be positive when it is compressive as in Fig. 1. However, since P can be either positive or negative, tension is also included.

The total potential energy, U and the kinetic energy, T of the axially loaded composite Timoshenko beam are given as follows [19]:

$$U = \frac{1}{2}\int_0^L \left\{EI_y(\theta')^2 - P[(w')^2 + (I_s/\mu)(\psi')^2] + 2K\theta'\psi' + kAG(w'-\theta)^2 + GJ(\psi')^2\right\} \mathrm{d}x, \tag{1a}$$

$$T = \frac{1}{2}\int_0^L [\mu(\dot{w})^2 + I_s(\dot{\psi})^2 + \rho I_y(\dot{\theta})^2] \, \mathrm{d}x, \tag{1b}$$

where primes and dots denote differentiation with respect to spanwise coordinate x and time t, respectively. Here ρ is the material density; A the cross sectional area; I_y the second moment of inertia of the beam cross section about the y-axis; $\mu = \rho A$ is the mass per unit length; I_s the polar mass moment of inertia per unit length about the x-axis; EI_y, GJ, K and kGA are the flexural rigidity, torsional rigidity, flexure–torsion coupling

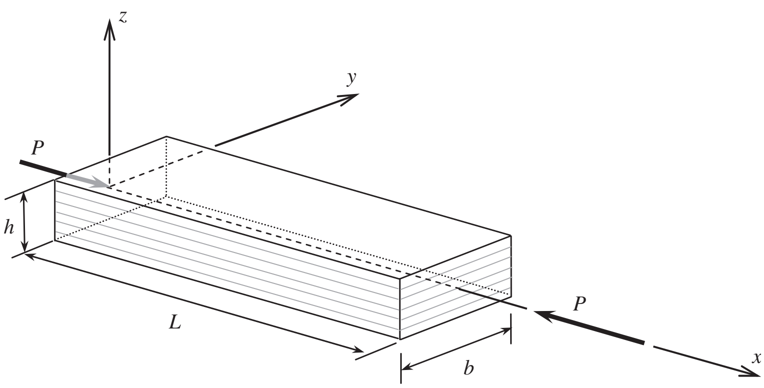

Fig. 1. Configuration of an axially loaded composite Timoshenko beam.

rigidity and shear rigidity of the composite beam, respectively. The expressions of the inertia and stiffness terms, i.e., ρI_y, μ, EI_y, etc., can be found in Song and Librescu [20].

Hamilton's principle, which is expressed as follows, is applied to the energy expressions given above in order to obtain the governing equations of motion and the boundary conditions:

$$\int_{t1}^{t2} (\delta T - \delta U + \delta W)\,\mathrm{d}t = 0. \tag{2}$$

Here, W is the virtual work done by the nonconservative forces. In this study, the virtual work and damping are not included. Therefore, substituting Eqs. (1a) and (1b) into Eq. (2) and knowing $\delta w = \delta\theta = \delta\psi = 0$ at $t = t_1$ and $t = t_2$, the following governing undamped partial differential equations of motion for the free vibration analysis of the beam model are obtained:

$$-\rho I\ddot{\theta} + EI_y\theta'' + kAG(w' - \theta) + K\psi'' = 0, \tag{3a}$$

$$-\mu\ddot{w} - Pw'' + kAG(w'' - \theta') = 0, \tag{3b}$$

$$-I_s\ddot{\psi} - P(I_s/\mu)\psi'' + K\theta'' + GJ\psi'' = 0. \tag{3c}$$

As a result of applying Hamilton's principle, the following boundary conditions are obtained:

- The geometric boundary conditions at the cantilever end, $x = 0$, of the Timoshenko beam:

$$w(0,t) = \theta(0,t) = \psi(0,t) = 0. \tag{4a}$$

- The natural boundary conditions at the free end, $x = L$, of the Timoshenko beam:

$$\text{Bending moment}: \quad EI_y\theta' + K\psi' = 0. \tag{4b}$$

$$\text{Shear force}: \quad -Pw' + kAG(w' - \theta) = 0. \tag{4c}$$

$$\text{Torque}: \quad -(PI_s/\mu)\psi' + K\theta' + GJ\psi' = 0. \tag{4d}$$

A sinusoidal variation of $w(x,t)$, $\psi(x,t)$ and $\theta(x,t)$ with a circular natural frequency ω is assumed and the functions are approximated as

$$w(x,t) = \bar{w}(x)\mathrm{e}^{\mathrm{i}\omega t}, \tag{5a}$$

$$\psi(x,t) = \bar{\psi}(x)\mathrm{e}^{\mathrm{i}\omega t}, \tag{5b}$$

$$\theta(x,t) = \bar{\theta}(x)\mathrm{e}^{\mathrm{i}\omega t}. \tag{5c}$$

Substituting Eqs. (5a)–(5c) into Eqs. (3a)–(3c), equations of motion can be rewritten as follows:

$$\rho I\omega^2\bar{\theta} + EI_y\bar{\theta}'' + kAG(\bar{w}' - \bar{\theta}) + K\bar{\psi}'' = 0, \tag{6a}$$

$$\mu\omega^2\bar{w} - P\bar{w}'' + kAG(\bar{w}'' - \bar{\theta}') = 0, \tag{6b}$$

$$I_s\omega^2\bar{\psi} - P(I_s/\mu)\bar{\psi}'' + K\bar{\theta}'' + GJ\bar{\psi}'' = 0. \tag{6c}$$

The following dimensionless parameters are introduced to make comparisons with the results in open literature:

$$\bar{x} = \frac{x}{L}, \quad \tilde{w} = \frac{\bar{w}}{L}, \quad r^2 = \frac{I}{AL^2}. \tag{7}$$

Using the parameters given above, Eqs. (6a)–(6c) can be expressed in the following dimensionless forms:

$$A_1\bar{\theta}^{**} + A_2\bar{\theta} + A_3\tilde{w}^{*} + A_4\bar{\psi}^{**} = 0, \tag{8a}$$

$$B_1\tilde{w}^{**} + B_2\tilde{w} + B_3\bar{\theta}^{*} = 0, \tag{8b}$$

$$C_1\bar{\psi}^{**} + C_2\bar{\psi} + C_3\bar{\theta}^{**} = 0, \tag{8c}$$

where $(\,)^* = \mathrm{d}(\,)/\mathrm{d}\bar{x}$ and $(\,)' = (1/L)(\,)^*$. Here, the dimensionless coefficients are:

$$A_1 = 1, \quad A_2 = \frac{\mu L^4 r^2}{EI_y}\omega^2 - \frac{kAGL^2}{EI_y}, \quad A_3 = \frac{kAGL^2}{EI_y}, \quad A_4 = \frac{K}{EI_y}, \tag{9a}$$

$$B_1 = 1 - \frac{P}{kAG}, \quad B_2 = \frac{L^2\mu}{kAG}\omega^2, \quad B_3 = -1 \tag{9b}$$

$$C_1 = 1 - \frac{PI_s}{GJ\mu}, \quad C_2 = \frac{I_s L^2}{GJ}\omega^2, \quad C_3 = \frac{K}{GJ}. \tag{9c}$$

Moreover, using the dimensionless parameters, the boundary conditions expressed in Eqs. (4a)–(4d) for $\bar{x} = 0$ and $\bar{x} = 1$ can be rewritten as follows:

$$\text{at } \bar{x} = 0 \Rightarrow \bar{\theta} = \tilde{w} = \bar{\psi} = 0, \tag{10a}$$

$$\text{at } \bar{x} = 1 \Rightarrow A_4\bar{\psi}^{*} + \bar{\theta}^{*} = 0, \tag{10b}$$

$$B_1\tilde{w}^{*} - \bar{\theta} = 0, \tag{10c}$$

$$C_1\bar{\psi}^{*} + C_3\bar{\theta}^{*} = 0. \tag{10d}$$

3. The differential transform method

The DTM is a transformation technique based on the Taylor series expansion and it is a useful tool to obtain analytical solutions of differential equations. In this method, certain transformation rules are applied and the governing differential equations and the boundary conditions of the system are transformed into a set of algebraic equations in terms of the differential transforms of the original functions and the solution of these algebraic equations gives the desired solution of the problem. It is different from high-order Taylor series method because Taylor series method requires symbolic computation of the necessary derivatives of the data functions and is expensive for large orders. The DTM is an iterative procedure to obtain analytic Taylor series solutions of differential equations. The basic definitions and the application procedure of this method can be introduced as follows.

Consider a function $f(x)$ which is analytic in a domain D and let $x = x_0$ represent any point in D. The function $f(x)$ is then represented by a power series whose centre is located at x_0. The differential transform of the function $f(x)$ is given by

$$F[k] = \frac{1}{k!}\left(\frac{\mathrm{d}^k f(x)}{\mathrm{d}x^k}\right)_{x=x_0}, \tag{11}$$

where $f(x)$ is the original function and $F[k]$ the transformed function.

The inverse transformation is defined as follows:

$$f(x) = \sum_{k=0}^{\infty}(x - x_0)^k F[k]. \tag{12}$$

Table 1
DTM theorems used for equations of motion

Original function	Transformed function
$f(x) = g(x) \pm h(x)$	$F[k] = G[k] \pm H[k]$
$f(x) = \lambda g(x)$	$F[k] = \lambda G[k]$
$f(x) = g(x)h(x)$	$F[k] = \sum_{l=0}^{k} G[k-l]H[l]$
$f(x) = \dfrac{d^n g(x)}{dx^n}$	$F[k] = \dfrac{(k+n)!}{k!} G[k+n]$
$f(x) = x^n$	$F[k] = \delta(k-n) = \begin{cases} 0 \text{ if } k \neq n, \\ 1 \text{ if } k = n. \end{cases}$

Table 2
DTM theorems used for boundary conditions

$x = 0$		$x = 1$	
Original B.C.	Transformed B.C.	Original B.C.	Transformed B.C.
$f(0) = 0$	$F(0) = 0$	$f(1) = 0$	$\sum_{k=0}^{\infty} F(k) = 0$
$\dfrac{df}{dx}(0) = 0$	$F(1) = 0$	$\dfrac{df}{dx}(1) = 0$	$\sum_{k=0}^{\infty} kF(k) = 0$
$\dfrac{d^2 f}{dx^2}(0) = 0$	$F(2) = 0$	$\dfrac{d^2 f}{dx^2}(1) = 0$	$\sum_{k=0}^{\infty} k(k-1)F(k) = 0$
$\dfrac{d^3 f}{dx^3}(0) = 0$	$F(3) = 0$	$\dfrac{d^3 f}{dx^3}(1) = 0$	$\sum_{k=0}^{\infty} (k-1)(k-2)kF(k) = 0$

Combining Eqs. (11) and (12), we get

$$f(x) = \sum_{k=0}^{\infty} \frac{(x - x_0)^k}{k!} \left(\frac{d^k f(x)}{dx^k} \right)_{x=x_0}. \tag{13}$$

Considering Eq. (13), it is noticed that the concept of differential transform is derived from Taylor series expansion. However, the method does not evaluate the derivatives symbolically.

In actual applications, the function $f(x)$ is expressed by a finite series and Eq. (13) can be rewritten as follows:

$$f(x) = \sum_{k=0}^{m} \frac{(x - x_0)^k}{k!} \left(\frac{d^k f(x)}{dx^k} \right)_{x=x_0}, \tag{14}$$

which means that $f(x) = \sum_{k=m+1}^{\infty} ((x - x_0)^k / k!)((d^k f(x)^k)/dx^k)_{x=x_0}$ is negligibly small. Here, the value of m depends on the convergence of the natural frequencies.

Theorems that are frequently used in the transformation of the differential equations and the boundary conditions are introduced in Tables 1 and 2, respectively.

4. Formulation with DTM

In the solution step, the DTM is applied to Eqs. (8a)–(8c) by using the theorems introduced in Table 1 and the following expressions are obtained:

$$A_1(k+2)(k+1)\theta[k+2] + A_2\theta[k] + A_3(k+1)W[k+1] + A_4(k+2)(k+1)\psi[k+2] = 0, \tag{15a}$$

$$B_1(k+2)(k+1)W[k+2]+B_2W[k]+B_3(k+1)\theta[k+1]=0, \tag{15b}$$

$$C_1(k+2)(k+1)\psi[k+2]+C_2\psi[k]+C_3(k+2)(k+1)\theta[k+2]=0, \tag{15c}$$

where $\theta[k]$, $W[k]$ and $\psi[k]$ are the transformed functions of $\bar{\theta}$, $\tilde{w}$, $\bar{\psi}$, respectively.

Additionally, applying DTM to Eqs. (10a)–(10d) by using the theorems introduced in Table 2, the boundary conditions are given as follows:

$$\text{at } \bar{x}=0 \Rightarrow \theta[0]=W[0]=\psi[0]=0, \tag{16a}$$

$$\text{at } \bar{x}=1 \Rightarrow A_4(k+1)\psi[k+1]+(k+1)\theta[k+1]=0, \tag{16b}$$

$$B_1(k+1)w[k+1]-\theta[k]=0, \tag{16c}$$

$$C_1(k+1)\psi[k+1]+C_3(k+1)\theta[k+1]=0. \tag{16d}$$

Substituting the boundary conditions expressed in Eqs. (16a)–(16d) into Eqs. (15a)–(15c) and taking $\theta[1]=c_1$, $W[1]=c_2$, $\psi[1]=c_3$, the following expression is obtained:

$$A_{j1}^{(n)}(\omega)c_1+A_{j2}^{(n)}(\omega)c_2+A_{j3}^{(n)}(\omega)c_3=0, \quad j=1,2,3, \tag{17}$$

where c_1, c_2 and c_3 are constants and $A_{j1}^{(n)}(\omega), A_{j2}^{(n)}(\omega), A_{j3}^{(n)}(\omega)$ are polynomials of ω corresponding to n.

The matrix form of Eq. (17) can be written as

$$\begin{bmatrix} A_{11}^{(n)}(\omega) & A_{12}^{(n)}(\omega) & A_{13}^{(n)}(\omega) \\ A_{21}^{(n)}(\omega) & A_{22}^{(n)}(\omega) & A_{23}^{(n)}(\omega) \\ A_{31}^{(n)}(\omega) & A_{32}^{(n)}(\omega) & A_{33}^{(n)}(\omega) \end{bmatrix} \begin{Bmatrix} c_1 \\ c_2 \\ c_3 \end{Bmatrix} = \begin{Bmatrix} 0 \\ 0 \\ 0 \end{Bmatrix}. \tag{18}$$

The eigenvalues are calculated by taking the determinant of the $\lfloor A_{ji} \rfloor$ matrix:

$$\begin{vmatrix} A_{11}^{(n)}(\omega) & A_{12}^{(n)}(\omega) & A_{13}^{(n)}(\omega) \\ A_{21}^{(n)}(\omega) & A_{22}^{(n)}(\omega) & A_{23}^{(n)}(\omega) \\ A_{31}^{(n)}(\omega) & A_{32}^{(n)}(\omega) & A_{33}^{(n)}(\omega) \end{vmatrix} = 0. \tag{19}$$

Solving Eq. (19), the eigenvalues are calculated. The jth estimated eigenvalue, $\omega_j^{(n)}$ corresponds to n and the value of n is determined by the following equation:

$$\left|\omega_j^{(n)}-\omega_j^{(n-1)}\right| \leqslant \varepsilon, \tag{20}$$

where $\omega_j^{(n-1)}$ is the jth estimated eigenvalue corresponding to $n-1$ and where ε is the tolerance parameter.

If Eq. (20) is satisfied, then the jth eigenvalue, $\omega_j^{(n)}$, is obtained. In general, $\omega_j^{(n)}$ are conjugated complex values, and can be written as $\omega_j^{(n)}=a_j+ib_j$. Neglecting the small imaginary part b_j, the jth natural frequency, a_j, is found.

After calculating the natural frequencies, the mode shapes can be plotted. The procedure used in plotting the mode shapes are explained below.

Using Eq. (18), the following equalities can be written:

$$A_{12}(\omega)c_2+A_{13}(\omega)c_3=-A_{11}(\omega)c_1, \tag{21a}$$

$$A_{22}(\omega)c_2+A_{23}(\omega)c_3=-A_{21}(\omega)c_1. \tag{21b}$$

Considering Eqs. (21a) and (21b), constants c_2 and c_3 can be written in terms of c_1 as follows:

$$c_2=-\frac{\begin{vmatrix} A_{11}(\omega) & A_{13}(\omega) \\ A_{22}(\omega) & A_{23}(\omega) \end{vmatrix}}{\Delta}c_1, \tag{22a}$$

$$c_3 = -\frac{\begin{vmatrix} A_{12}(\omega) & A_{11}(\omega) \\ A_{22}(\omega) & A_{21}(\omega) \end{vmatrix}}{\Delta} c_1, \tag{22b}$$

where

$$\Delta = \begin{vmatrix} A_{12} & A_{13} \\ A_{22} & A_{23} \end{vmatrix}. \tag{23}$$

The functions $\bar{\theta}(\bar{x})$, $\tilde{w}(\bar{x})$ and $\bar{\psi}(\bar{x})$ are expressed in series as explained before in DTM application so they can be written as follows:

$$\bar{\theta}(\bar{x}) = \sum_{k=1}^{m} \theta[k]\bar{x}^k, \tag{24a}$$

$$\tilde{w}(\bar{x}) = \sum_{k=1}^{m} W[k]\bar{x}^k, \tag{24b}$$

$$\bar{\psi}(\bar{x}) = \sum_{k=1}^{m} \psi[k]\bar{x}^k. \tag{24c}$$

Here the $\theta[k]$, $W[k]$ and $\psi[k]$ are the transformed functions of $\bar{\theta}$, $\tilde{w}$, $\bar{\psi}$ and they can be expressed in terms of ω, c_1, c_2 and c_3. Since c_2 and c_3 have been written in terms of c_1 above, $\theta[k]$, $W[k]$ and $\psi[k]$ can be expressed in terms of c_1 as follows:

$$\theta[k] = \theta(\omega, c_1), \tag{25a}$$

$$W[k] = W(\omega, c_1), \tag{25b}$$

$$\psi[k] = \psi(\omega, c_1). \tag{25c}$$

Using the functions given by Eqs. (25a)–(25c), the mode shapes can be plotted for several values of ω.

5. Results and discussion

The computer package Mathematica is used to write a program for the expressions given by Eqs. (15a)–(16d). In order to validate the calculated results, illustrative examples, taken from Refs. [6,19], are solved and the results are compared with the ones given in these references.

The beam model studied in Ref. [6] is solved in this study as an illustrative example by using DTM. It is a cantilever glass-epoxy composite beam with a rectangular cross section with width = 12.7 mm and thickness = 3.18 mm. Unidirectional plies each having fibre angles of +15°are used in the analysis. The data used for the analysis are as follows:

$$EI = 0.2865\,\mathrm{N\,m^2},\quad GJ = 0.1891\,\mathrm{N\,m^2},\quad kAG = 6343.3\,\mathrm{N},$$
$$\mu = 0.0544\,\mathrm{kg/m},\quad I_s = 0.777\times10^{-6}\,\mathrm{kg\,m},\quad K = 0.1143\,\mathrm{N\,m^2},$$
$$L = 0.1905\,\mathrm{m},\quad r^2 = 0.00002322.$$

First, expressions for the second and third transformed functions of $\bar{\theta}$, $\tilde{w}$, $\bar{\psi}$ are given below by allowing the axial force, P, as a variable:

$$\theta[2] = \frac{(0.121378P - 1606.98)c_2}{3.03542 - 0.000302128P},$$

$$\theta[3] = \frac{3.56938\times10^{-7}c_3\omega^2 + 6c_1(1 - 0.0000755319P)\big((0.126668P/0.000157647P - 1) - 5.80653\times10^{-9}\omega^2\big)}{27.3188 - 0.00271915P},$$

$$W[2] = \frac{0.5c_1}{1 - 0.000157647P},$$

$$W[3] = \frac{2.09954 \times 10^7 c_2(-535.66 - 1.5745 \times 10^{-7}\omega^2 + P(0.0404594 + 1.56716 \times 10^{-11}\omega^2))}{(P - 10046.8)(P - 6343.3)},$$

$$\psi[2] = \frac{971.327c_2}{3.03542 - 0.000302128P},$$

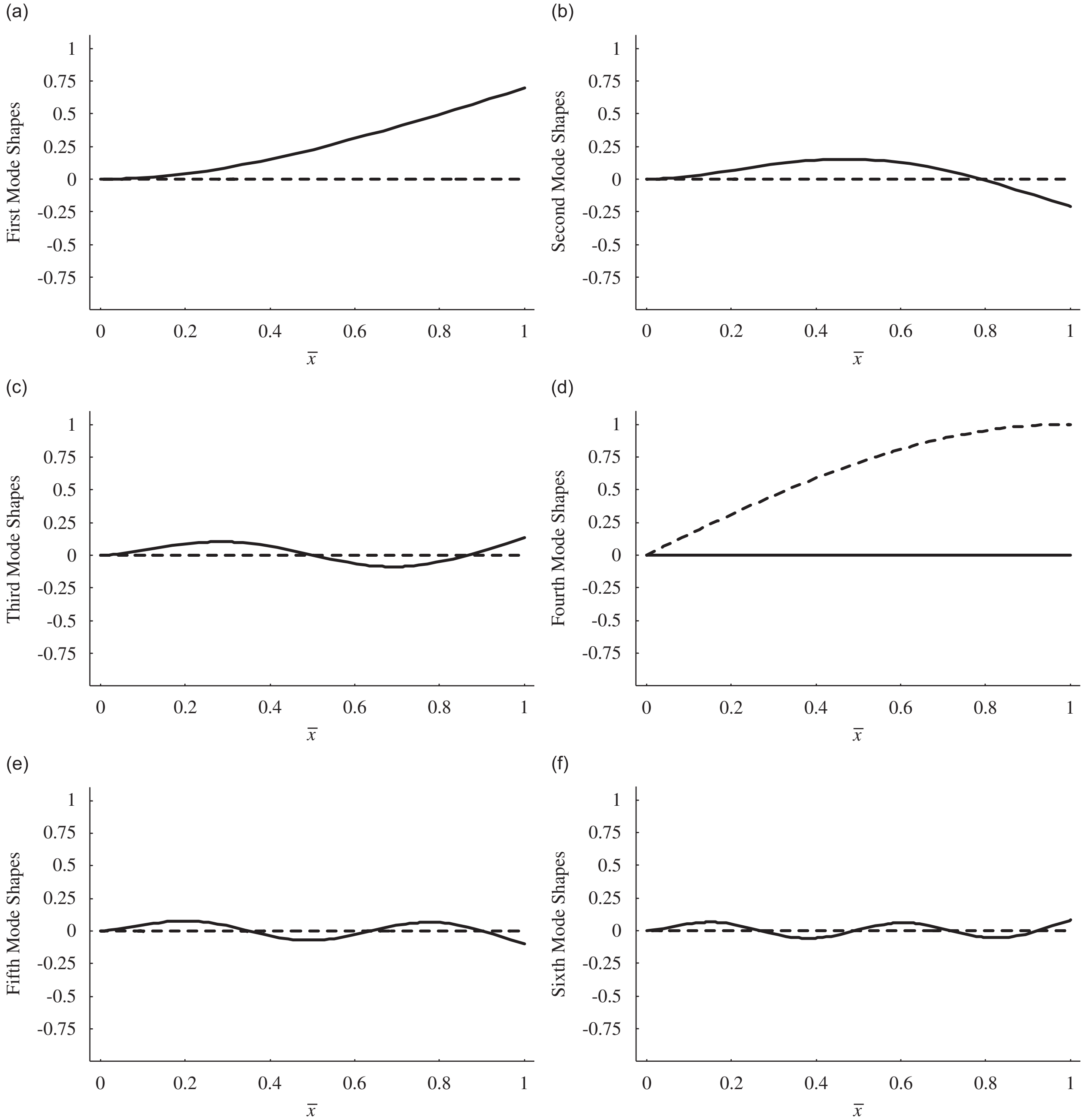

Fig. 2. (a–f) The normal mode shapes of the composite beam without bending–torsion coupling (——, w; - - -, ψ).

$$\psi[3]=\frac{c_1(1.07165\times10^6P+0.0491252\omega^2-7.74443\times10^{-6}P\omega^2)+c_3\omega^2(0.000329032P-2.08715)}{6.373\times10^7-16390.1P+P^2}.$$

In Fig. 2(a)–(f), the first six mode shapes of the considered beam model under the effect of the compressive axial force ($P=7.5$) are introduced without coupling. Additionally, the same mode shapes are plotted in Fig. 3(a)–(f) by including the coupling effect. When Figs. 2 and 3 are compared with the ones in Ref. [19], it is seen that the results are in good agreement. Fig. 2(a)–(f) reveal that the first three, the fifth and the sixth normal modes are bending modes while the fourth normal mode is the fundamental torsion mode. Fig. 3(a)–(f)

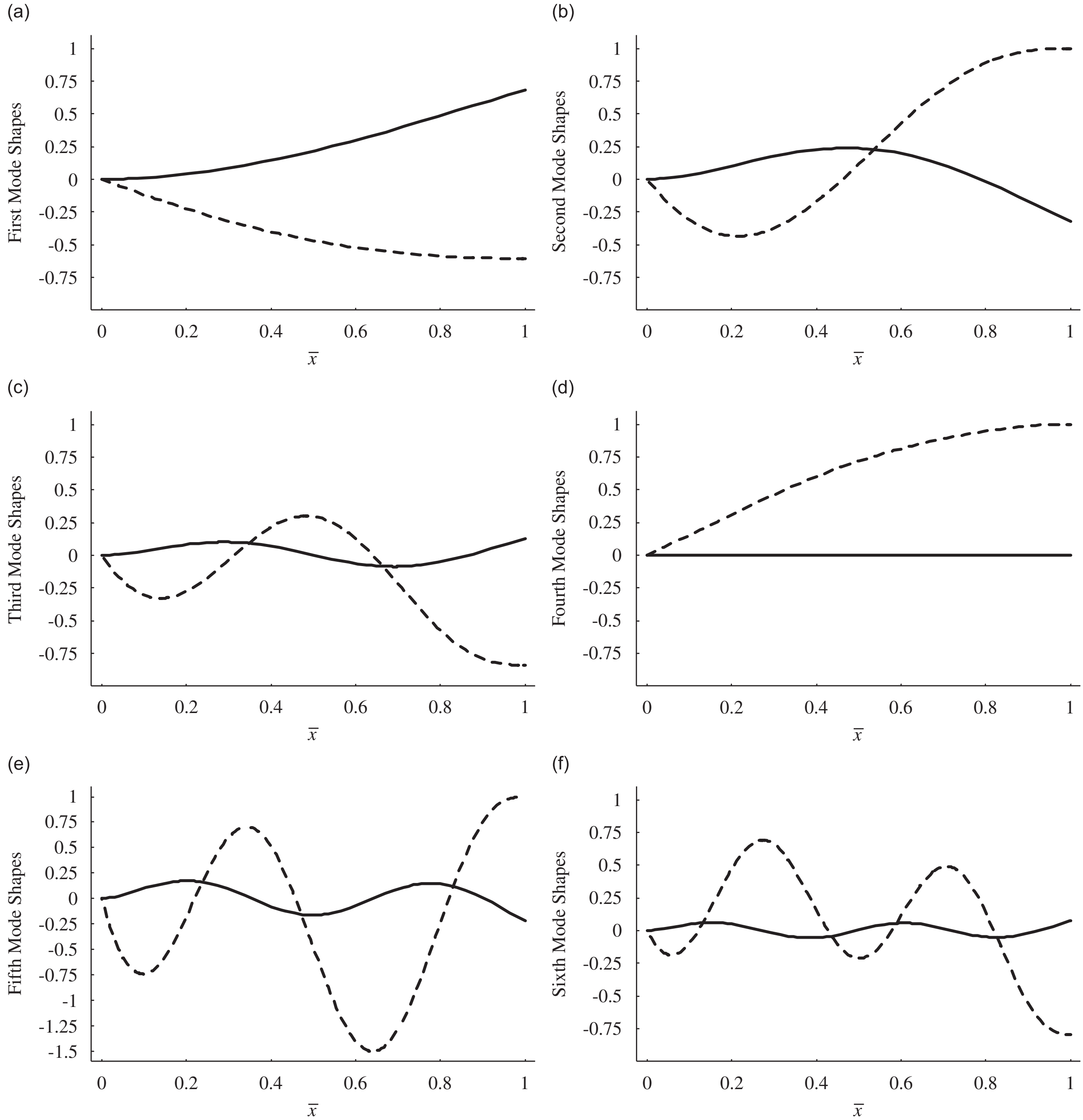

Fig. 3. (a–f) The sixth normal mode shapes of the composite beam with bending–torsion coupling (——, w; - - -, ψ).

Table 3
Effects of axial force and bending-torsion coupling on the natural frequencies

Natural frequencies											
$P = 7.5$ (compression)				$P = 0$				$P = -7.5$ (tension)			
Coupled		Uncoupled		Coupled		Uncoupled		Coupled		Uncoupled	
DTM	Ref. [6]	DTM	Ref. [19]	DTM	Ref. [6]	DTM		DTM	Ref. [6]	DTM	Ref. [19]
21.987	21.99	28.064	28.06	30.747	30.75	35.283		37.106	37.1	40.975	40.97
181.495	181.5	210.162	210.16	189.779	189.8	217.341		197.672	197.7	224.259	224.25
511.818	511.9	586.519	586.51	518.791	518.8	592.626		525.665	525.6	598.668	598.66
648.047	648.0	647.228	647.22	648.169	648.3	647.411		648.495	648.6	647.595	647.59
979.473	–	1113.950	1113.95	986.199	–	1119.847		992.878	–	1125.711	1125.71
1558.134	–	1766.662	–	1564.751	–	1772.556		1571.338	–	1778.429	–

Table 4
Effects of the inverse of the slenderness ratio on the natural frequencies

r	Natural frequencies					
0	21.98865	181.56047	512.22181	648.05015	980.76696	1560.98805
0.02	21.96686	180.44028	505.38498	647.99460	959.09075	1513.44841
0.04	21.90184	177.19537	486.33305	647.85277	901.14712	1390.13207
0.06	21.79469	172.14481	458.78059	476.56065	823.57290	1235.12260
0.08	21.64714	165.73826	427.12073	647.35065	742.62206	1085.00090
0.1	21.46153	158.46520	394.95017	645.81753	668.83578	954.67926

reveal that the first three, the fifth and the sixth normal modes are the coupled modes while the fourth normal mode remains the fundamental torsion mode.

In Table 3, effects of axial force and bending–torsion coupling on the natural frequencies are inspected. Here, the first six natural frequencies, calculated for the undamped vibration, are introduced and the results of Refs. [6 and 19] are given for comparison. When Table 3 is considered, it is noticed that the natural frequencies increase as the axial force changes from compression ($P = 7.5$) to tension ($P = -7.5$) which reveals that the compressive force has a softening effect on the natural frequencies while the tension force has a stiffening effect. Additionally, it is noticed that bending–torsion coupling has a decreasing effect on the natural frequencies. However, since the fourth normal mode is the fundamental torsion, it is normal that bending–torsion coupling and the value of the axial force have very little effect on the fourth natural frequency [6].

Effects of the inverse of the slenderness ratio, r, is investigated and the results are tabulated in Table 4. Here it is noticed that inverse of the slenderness has a decreasing effect on the natural frequencies. Therefore, the natural frequencies of a coupled Timoshenko beam are lower than the natural frequencies of a coupled Euler–Bernoulli beam. Additionally, it is observed that the decrease in the natural frequencies is more for the higher modes. The Timoshenko beam theory is mostly used when the higher modes are examined so it is something expected that Timoshenko effect is more dominant on the higher modes.

In Fig. 4, convergence of the first four natural frequencies are introduced. Here, it is seen that to evaluate up to fourth natural frequency to five-digit precision, it was necessary to take 34 terms. Therefore, the value of m mentioned in Eq. (14) is 34 for the first four natural frequencies. Additionally, here it is seen that higher modes appear when more terms are taken into account in DTM application. Thus, depending on the order of the required mode, one must try a few values for the term number at the beginning of the Mathematica calculations in order to find the adequate number of terms.

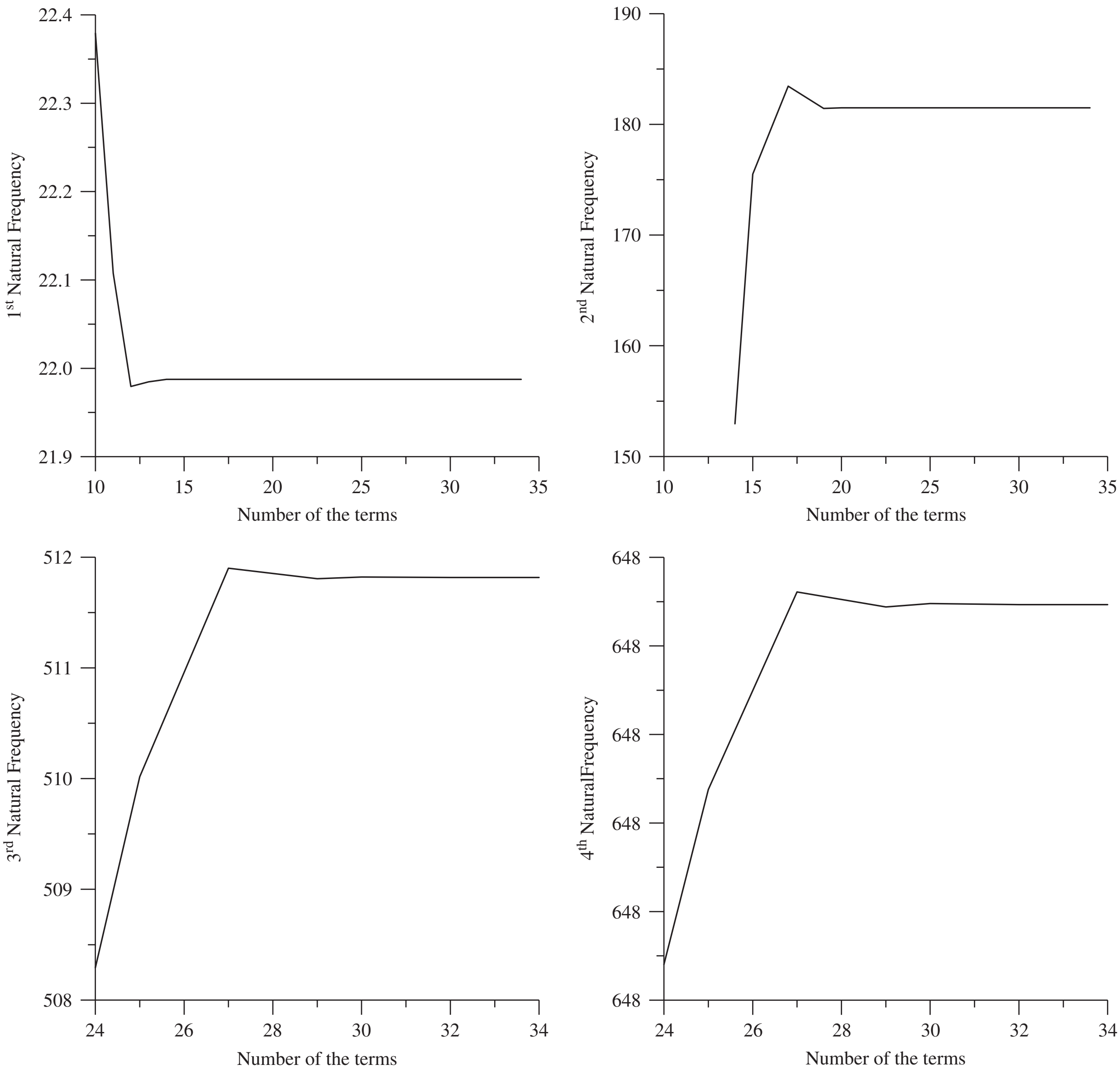

Fig. 4. Convergence of the first four natural frequencies.

6. Conclusion

Using Hamilton's principle, the equations of motion are derived for a cantilever composite Timoshenko beam featuring bending–torsion coupling and these equations are solved using the DTM. The essential steps of the DTM application includes transforming the governing equations of motion into algebraic equations, solving the transformed equations and then applying a process of inverse transformation to obtain any desired natural frequency. All the steps are very straightforward. At first glance, application of the DTM to both the equations of motion and the boundary conditions seem to be very involved computationally. However, all the algebraic calculations are finished quickly by using a symbolic computational software. Besides all these, the analysis of the convergence of the results show that DTM solutions converge fast. When the results are compared with the published exact results, very good agreement is observed.

Additionally, the following results are obtained in this study:

- In the case of uncoupled modes, the first three, the fifth and the sixth normal modes are bending modes while the fourth normal mode is the fundamental torsion mode.
- In the case of coupled modes, the first three, the fifth and the sixth normal modes are the coupled modes while the fourth normal mode remains the fundamental torsion mode.
- The compressive force has a softening effect on the natural frequencies while the tension force has a stiffening effect so the natural frequencies increase as the axial force changes from compression to tension.
- Bending–torsion coupling has a decreasing effect on the natural frequencies.
- Inverse of the slenderness has a decreasing effect on the natural frequencies, especially on the higher modes.

References

[1] L. Jun, S. Rongying, H. Hongxing, J. Xianding, Bending–torsional coupled dynamic response of axially loaded composite Timoshenko thin-walled beam with closed cross-section, *Composite Structures* 64 (2004) 23–35.
[2] L. Jun, J. Xianding, Response of flexure–torsion coupled composite thin-walled beams with closed cross-sections to random load, *Mechanics Research Communications* 32 (2005) 25–41.
[3] L.C. Bank, C.H. Kao, Dynamic response of composite beam, in: D. Hui, J.R. Vinson, (Eds.), *Recent Advances in the Macro- and Micro-Mechanics of Composite Material Structures*, *AD 13*, *The Winter Annual Meeting of the 1975 ASME*, Chicago, IL, November–December 1977.
[4] O. Song, L. Librescu, Bending vibration of cantilevered thin-walled beams subjected to time-dependent external excitations, *Journal of the Acoustical Society of America* 98 (1995) 313–319.
[5] S.R. Rao, N. Ganesan, Dynamic response of non-uniform composite beams, *Journal of Sound and Vibration* 200 (1997) 563–577.
[6] J.R. Banerjee, Free vibration of axially loaded composite Timoshenko beams using the dynamic stiffness matrix method, *Computers and Structures* 69 (1998) 197–208.
[7] S. Na, L. Librescu, Dynamic response of elastically tailored adaptive cantilevers of non-uniform cross section exposed to blast pressure pulses, *International Journal of Impact Engineering* 25 (2001) 847–867.
[8] M.O. Kaya, Free vibration analysis of rotating Timoshenko beams by differential transform method, *Aircraft Engineering and Aerospace Technology: an International Journal* 78 (3) (2006) 194–203.
[9] O. Ozdemir Ozgumus, M.O. Kaya, Flapwise bending vibration analysis of double tapered rotating Euler–Bernoulli beam by using the differential transform method, *Meccanica* 41 (6) (2006) 661–670.
[10] Ö. Özdemir, M.O. Kaya, Flapwise bending vibration analysis of a rotating tapered cantilevered Bernoulli–Euler beam by differential transform method, *Journal of Sound and Vibration* 289 (2006) 413–420.
[11] J.K. Zhou, *Differential Transformation and its Application for Electrical Circuits*, Huazhong University Press, Wuhan, PR China, 1986.
[12] J.S. Chiou, J.R. Tzeng, Application of the Taylor transform to nonlinear vibration problems, transaction of the American Society of mechanical engineers, *Journal of Vibration and Acoustics* 118 (1996) 83–87.
[13] M.J. Jang, C.L. Chen, Y.C. Liu, Two-dimensional differential transform for partial differential equations, *Applied Mathematics and Computation* 121 (2001) 261–270.
[14] I.H. Abdel, H. Hassan, On solving some eigenvalue-problems by using a differential transformation, *Applied Mathematics and Computation* 127 (2002) 1–22.
[15] O. Ozdemir Ozgumus, M.O. Kaya, Formulation for flutter and vibration analysis of a hingeless helicopter blade in hover: part I, *Aircraft Engineering and Aerospace Technology* 79 (2) (2007) 177–183.
[16] O. Ozdemir Ozgumus, M.O. Kaya, Results of flutter stability and vibration analysis of a hingeless helicopter blade in hover: part II, *Aircraft Engineering and Aerospace Technology* 79 (3) (2007) 231–237.
[17] O. Ozdemir Ozgumus, M.O. Kaya, Energy expressions and free vibration analysis of a rotating double tapered Timoshenko beam featuring bending–torsion coupling, *The International Journal of Engineering Science*, doi:10.1016/j.ijengsci.2007.04.005.
[18] S. Catal, Analysis of free vibration of beam on elastic soil using differential transform method, *Structural Engineering and Mechanics* 24 (1) (2006) 51–62.
[19] J. Li, R. Shen, H. Hua, X. Jin, Bending–torsional coupled vibration of axially loaded composite Timoshenko thin-walled beam with closed cross-section, *Composite Structures* 64 (2004) 23–35.
[20] O. Song, L. Librescu, Free vibration of anisotropic composite thin-walled beams of closed cross-section contour, *Journal of Sound and Vibration* 167 (1993) 129–147.